Biochemical and Biophysical Research Communications 461 (2015) 268–274

Contents lists available at ScienceDirect

Biochemical and Biophysical Research Communications

journal homepage: www.elsevier.com/locate/ybbrc

Intensified autophagy compromises the efficacy of radiotherapy against prostate cancer

Michael I. Koukourakis [a, *], Dimitra Kalamida [a], Achilleas Mitrakas [a], Stamatia Pouliliou [a], Sofia Kalamida [a], Efthimios Sivridis [b], Alexandra Giatromanolaki [b]

[a] Department of Radiotherapy/Oncology, Democritus University of Thrace, Alexandroupolis, 68100, Greece
[b] Department of Pathology, Democritus University of Thrace, Alexandroupolis, 68100, Greece

ARTICLE INFO

Article history:
Received 28 March 2015
Available online 15 April 2015

Keywords:
Prostate cancer
Autophagy
LC3A
LAMP2a
Aggresomes
Radiotherapy

ABSTRACT

Introduction: Radiotherapy is an equivalent alternative or complement to radical prostatectomy, with high therapeutic efficacy. High risk patients, however, experience high relapse rates, so that research on radio-sensitization is the most evident route to improve curability of this common disease.
Materials and methods: In the current study we investigated the autophagic activity in a series of patients with localized prostate tumors treated with radical radiotherapy, using the LC3A and the LAMP2a proteins as markers of autophagosome and lysosome cellular content, respectively. The role of autophagy on prostate cancer cell line resistance to radiation was also examined.
Results: Using confocal microscopy on tissue biopsies, we showed that prostate cancer cells have, overall, high levels of LC3A and low levels of LAMP2a compared to normal prostate glands. Tumors with a 'highLC3A/lowLAMP2a' phenotype, suggestive of intensified lysosomal consumption, had a significantly poorer biochemical relapse free survival. The PC3 radioresistant cell line sustained remarkably its autophagic flux ability after radiation, while the DU145 radiosensitive one experiences a prolonged blockage of the autophagic process. This was assessed with aggresome accumulation detection and LC3A/LAMP2a double immunofluorescence, as well as with sequestrosome/p62 protein detection. By silencing the LC3A or LAMP2a expression, both cell lines became more sensitive to escalated doses of radiation.
Conclusions: High base line autophagy activity and cell ability to sustain functional autophagy define resistance of prostate cancer cells to radiotherapy. This can be reversed by blocking up-regulated components of the autophagy pathway, which may prove of importance in the field of clinical radiotherapy.

1. Introduction

Prostate cancer is one of the most common tumors in man. Radical prostatectomy or radiotherapy offer high cure rates, especially in early stages of the disease [1]. Extracapsular invasion, high Gleason score and high serum PSA levels, however, are linked with higher recurrence rates [2,3], and this group of patients consists of a major challenge in radiation oncology. Combined chemo-radiotherapy with currently available drugs is not recommended in the clinical routine, although proper randomized trials are missing. Targeting biological pathways active in such tumors is the only apparent route to anticipate encouraging steps for the development of more effective radiotherapy combinations.

DNA repair is certainly one of the exhaustively investigated pathways in the attempt to develop agents that could promote post-irradiation cell death [4]. Cytoplasmic membranes and organelles, although damaged by ionizing radiation, have not focused proper attention. Autophagy is a major pathway involved in the degradation and recycling of long lived and damaged proteins and organelles [5]. The target material becomes engulfed in autophagosomal membranes and, following auto-lysosomal fusion, this is digested by the lysosomal hydrolases. Degraded products are rendered to the cell for further metabolic usage. As irradiation loads the cell with damaged proteins and membranes, autophagy is essential for the cell to get rid of waist material. Moreover, the re-usage of degraded molecules, given also the austerity conditions that prevail in the tumor body, certainly provides a survival advantage [6].

* Corresponding author. Department of Radiotherapy/Oncology, Democritus University of Thrace, PO BOX 12, Alexandroupolis 68100, Greece. Fax: +30 25510 30349.
E-mail address: targ@her.forthnet.gr (M.I. Koukourakis).

http://dx.doi.org/10.1016/j.bbrc.2015.04.014
0006-291X/

Microtubule associated protein 1 – LC3A is a structural component of the autophagosomal membrane. LC3A-I is the soluble form which, following its conjugation to the head group amine of phosphatidylethanolamine, is transformed to the LC3A-II form that resides on autophagosome membranes [5]. On the other hand, LAMP2a is a structural lysosomal protein residing on lysosomal membranes [7]. Using double immunofluorescence, with antibodies specific for these two proteins, and confocal microscopy we investigated the auto-lysosomal flux in cancer biopsies from prostate cancer patients treated with radical radiotherapy and its eventual role in radioresistance. In vitro experiments with prostate cancer cells lines have been also performed to assess their autophagic response and the eventual role of LC3A and LAMP2a protein repression in sensitizing cells to radiation.

2. Materials and methods

Archived formalin-fixed paraffin-embedded tissues from 12 non-malignant prostate biopsies and 54 biopsy specimens from prostate cancer patients were retrieved from our pathology department. Patients were consecutive according to their radiotherapy referral number, to avoid selection bias. The study has been approved by the Local Research and Ethics Committee. All cancer patients had been treated with radical hypofractionated and accelerated radiotherapy (with or without androgen deprivation). Details on the technique of radiotherapy have been previously reported [8]. Briefly, a total of 15 fractions or 3.5 Gy are delivered within 19 days to the prostate and seminal vesicles. Patients with PSA > 10 ng/ml or Gleason score ≥7 also receive pelvic irradiation (concomitant boost technique: 2.7 Gy × 14 fractions to the pelvis and 0.8 Gy to the prostate and seminal vesicles, followed by a 15th fraction of 3.5 Gy confined to the prostate area).

Patient characteristics are shown in Table 1. Out of 54 cases 17 were of T1-stage, 31 of T2-stage and 6 had extra-capsular or seminal vesicle extension (T3-stage). The above staging was based on biopsy, and CT/MRI pelvic imaging. Patients with radiologically confirmed enlarged nodes were excluded. The Gleason score ranged from 4 to 10 (median 5). A low Gleason score of 4–6 characterized 33/54 (61%) cases, a high score of 7–10 characterized 21/54 (39%) cases. Pre-radiotherapy maximum PSA levels were also available, ranging from 4.3 to 52 (median 11.7).

The median follow up of patients treated with radiotherapy was 36 months (range 6–75). PSA levels were assessed every 6-months and the biochemical relapse free survival (BRFS) interval was assessed for analysis.

Table 1
Patient and disease characteristics.

No pts	54
Age	Median 69
	Range 52–77
T-stage	
T1	17
T2	31
T3[a]	6
Node involvement[a]	
No	54
Yes	0
Gleason score	
4–7	33
7–10	21
PSA levels	
5.0–10	24
>10	30

[a] CT/MRI assessment.

2.1. Tissues immunofluorescence protocol

Sections were cut at 3 μm from formalin-fixed paraffin-embedded tissues and dried for 30 min at 80 °C and mounted on poly-L-lysin coated slides. Following deparaffinization and rehydration, slides were incubated thrice, at 120 °C for 5 min. Hyperoxidase blockage followed at room temperature. The Ultra Vision Quanto-HRP THERMO-kit (THERMO FISHER SCIENTIFIC) was used for immunohistochemistry. The samples were then stained with a sequential immunofluorescence staining protocol for both LC3A and LAMP2A proteins. Anti-LC3A, rabbit polyclonal, primary antibody (1:200, Abcam) was firstly incubated for 1 h at room temperature. The slides were then washed in PBS pH 7.4, incubated with the appropriate CF 488 secondary antibody (1:250; Biotium) for 30 min at room temperature, followed by PBS washes. The samples were then blocked in PBS/5% w/v BSA pH 7.4 for 20 min, and the second step of the sequential staining was performed with anti-LAMP2A rabbit polyclonal, primary antibody (1:100, Abcam) for 1 h at room temperature. The slides were then washed in PBS pH 7.4, incubated with the appropriate CF 564 secondary antibody (1:250; Biotium) and the DNA was counterstained with Hoechst 33342 (1 μg/ml; Sigma–Aldrich) for 30 min at room temperature. After final washes with PBS, coverslips were mounted on the top of the samples using homemade Mowiol mounting medium.

2.2. Detection of aggresomes

Aggresome visualization has been performed using the Proteo-Stat® Aggresome detection kit for fluorescence microscopy (Enzo Life Sciences LTD, UK) according to the manufacturer's instructions. Aggresome accumulation can directly linked to the inhibition of autophagy, and especially the inhibition of the “autophagic flux”. MG132, a proteasome inhibitor, promoting aggresome accumulation has been used as a positive control, while the nuclei have been counterstained using Hoechst 33342, both provided by the kit. The stained samples have been imaged by confocal microscopy with ×100 magnification using a standard red filter (561 nm). PC3 and DU145 prostate cancer cell lines have been irradiated with 8Gy and 4Gy respectively, aggresomes have been detected two days following radiation, and non-irradiated cells have been used as control.

2.3. Confocal microscopy and image analysis

Imaging was performed on a customized Andor Revolution Spinning Disk Confocal System built around a stand (IX81; Olympus) with a 60× lens and a digital camera (Andor Ixon+885) (CIBIT Facility, MBG-DUTH). Image acquisition was performed in Andor IQ 2 software. Optical sections were recorded every 0.3 μm.

Image intensity analysis for the obtained data sets has been performed using ImageJ 1.47v (National Institute of Health, USA) software. Image processing macros have been custom developed in order to quantify the levels of the examined proteins in the area of interest. The two-dimensional (2D) average projection of z-stack images were quantified using a standard size square area, where integrated intensity values have been measured. Co-localization analysis was also performed and the Pearson's co-efficient for each image was calculate using the Coloc2 plugin in ImageJ. Graph presentation has been performed using the GraphPad Prism Version 5.01a statistical package (GraphPad Software Inc., USA).

2.4. Western blot analysis

Whole fraction of cell lysates separated on discontinuous SDS gels using 8% separating gel for LAMP2a and 12.5% for LC3A

separating gel. Moreover, 5% stacking gel was used. Forty nanograms of samples analyzed on the gel. Immunoblotting was performed utilizing PVDF-PSQ membranes (Millipore Corp.). Then, membranes were blocked with 5% non-fat dry milk in 150 mM NaCl, 10 mM Tris, pH 7.5 (TBS) and 0.1% (v/v) Tween-20 at room temperature for 2 h followed by the hybridization overnight at 4 °C with primary antibodies. The membranes were then hybridized for 2 h at room temperature with the secondary antibody, goat polyclonal to rabbit IgG-HRP (1:3.000, Biorad, 1706515, USA) or goat polyclonal to mouse IgG-HRP (1:3.000, Biorad, 1706516, USA). Bands were developed using Chemidoc MP Imaging System (Biorad, USA).

The primary antibodies used were: the rabbit polyclonal to LC3A (1:1.000, ab62720, Abcam), the rabbit polyclonal antibody to LAMP2a (1:1.000, ab18528, Abcam) and the rabbit polyclonal antibody to SQSTM1/p62 (1:1.000, ab64134, Abcam). Each of these blots was then stripped, dried overnight, re-hybridized with a mouse polyclonal antibody to tubulin (dilution 1:10.000; Mouse Monoclonal Anti-α-Tubulin T9026; Sigma).

2.5. Cell cultures and gene silencing

DU145 and PC3 prostate cell lines were cultured, using DMEM basal medium (31885-023, Gibco) at 37 °C, 5% CO_2. LC3A siRNAs were pooled as (5′-GCGAGUUGGUCAAGAUCAUTT-3′), (5′-GCUUCCUCUAUAUGGUCUATT-3′), (5′-CCUGCUGUGUGGUUCAUCUTT-3′), (5′-GCUGUAAGGAGGUACAGCATT-3′), and LAMP2A siRNA were respectively pooled as (5′-GCAGUGCAGAUGACGACAATT-3′), (5′-GCACCAUCAUGCUG-GAUAUTT-3′), (5′-CCCAGUGUCAUUAGAUAAUTT-3′), (5′-GGCUACAACAG-AACUUAAATT-3′). These were custom synthesized from Shanghai GenePharma Co., Ltd (China). The siRNAs were used at 50 nM and 100 nM for LC3A and LAMP2A respectively, to transfect cells using HiPerfect (QIAGEN) according to the manufacturer's instructions for 24 h, while the silencing efficiency of siRNAs was confirmed both by confocal microscopy and western blot after 24 h.

2.6. Post-irradiation viability experiments

After silencing of LC3A and LAMP2a, control and silenced PC3 and DU145 cell lines were treated with multi-dose of radiation. Seven days later the cell viability was measured using AlamarBlue® assay which constitutes a method based on the metabolic activity of cells to reduce resazurin (oxidized form; 7-hydroxy-3H-phenoxazin-3-1-10-oxide) to resorufin. This counts the number of cells with active mitochondria, given that resazurin reduction is performed by mitochondrial enzymes [9]. 250 cells/well were plated in a 96-well plate and 10% v/v of AlamarBlue® was added in each well. After a 7-h incubation fluorescence was measured using 590 nm as emission wavelength and 530–560 nm as excitation wavelength. Moreover, we used culture medium as negative control while vitamin C was used as positive control for the full reduction of resazurin. The relative fluorescence units and the absolute % Alamar Blue® reduction were as previously described [9]. Experiments were performed in six wells for each dose level and cell condition.

2.7. Statistical analysis

The statistical analysis and graph presentation was performed using the GraphPad Prism 5.00 version (san Diego, CA). The Fisher's exact test was used to compare categorical variables. Survival curves were plotted using the Kaplan–Meier method, and the log-rank test was used to determine statistical differences between life tables. A Cox proportional hazard model was used to further test the independent significance of variables. For cell viability experiments, comparison of fluorescence counts at the applied dose levels was performed using the unpaired-two-tailed t-test. p values < 0.05 were considered to be statistically significant.

3. Results

3.1. Tissue expression patterns

The epithelium of the normal prostate glands showed a strong expression of the LAMP2a protein, while low levels of the LC3A were evident (Fig. 1A1,2). On the contrary, LC3A was overexpressed in cancer cells, in most cases examined, while LAMP2a expression was significantly reduced compared to normal prostate epithelium (Fig. 1B).

Analysis of the fluorescence intensity FI data obtained in confocal microscopy confirmed this observation (Fig. 1C). The median LC3A FI was 4.13 (range 3.53–4.54) in the normal prostate epithelium vs. 5.31 (range 2.46–14.57) in the cancer epithelium ($p = 0.0001$). The median LAMP2a FI was 5.21 (range 4.36–5.49) in the normal prostate epithelium vs. 2.93 (range 1.41–9.58) in the cancer epithelium ($p < 0.0001$). Colocalization between the two proteins, indicative of auto-lysosomes, had a similar median Pearson's coefficient ($p = 0.41$).

3.2. Correlation with histopatholgical variables

Analysis of the FI did not confirm any association of the above parameters with T-stage or the Gleason score. However, combined analysis showed that tumors with low LC3A and high LAMP2a expression, a pattern resembling to the normal prostate expression one, had a significantly lower Gleason score ($p = 0.04$). On the other hand, tumors with high pre-radiotherapy serum PSA levels (>15 mg/ml) showed a higher LC3A/LAMP2a co-localization Pearson's score (0.52 vs. 0.44; $p = 0.009$). There was no association of MIB1 proliferation index (data not shown).

3.3. Biochemical relapse free survival

Using the median value of the three auto-lysosomal parameters, patients were classified in two groups (low vs. high). Kaplan–Meier BRFS curves showed that high LC3A and low LAMP2a expression were linked with poor post-radiotherapy outcome ($p = 0.01$ and $p = 0.0008$, respectively); Fig. 2A and B. Combined LC3A/LAMP2a analysis showed that cases with high LC3A and low LAMP2a had the poorest BRFS ($p = 0.0001$) Fig. 2C. No association with PC was noted ($p = 0.24$) Fig. 2D. In multivariate analysis, including T-stage and Gleason score, only LAMP2a was revealed as an independent prognostic variable ($p = 0.02$, hazard ratio 6.04).

3.4. Effect of RT on autophagic flux in cancer cell lines

The effect of 4 Gy and 8 Gy of irradiation on the autophagic flux of DU145 (radiosensitive) and the PC3 (radioresistant) prostate cancer cell lines, respectively, was assessed with confocal microscopy and the aggresome detection method. Blockage of the proteasome pathway using the MG132 blocker sharply induced the accumulation of undigested aggresomes in both cell lines (Fig. 3). Irradiation of DU145 cells with 4 Gy resulted in intense accumulation of aggresomes 2 days (Fig. 3A), and further experiments suggested that this is extended at least up to 7 days after irradiation (data not shown). On the contrary, PC3 cells sustained their autophagic flux unaltered (Fig. 3B).

Double immunostaining with LC3A/LAMP2a showed a marked reduction of LC3A/LAMP2a colocalization in the DU145 cell line at 2 days after irradiation, while colocalization was intensified in the PC3 cell line (Fig. 3A and B). At this time point, western blot analysis

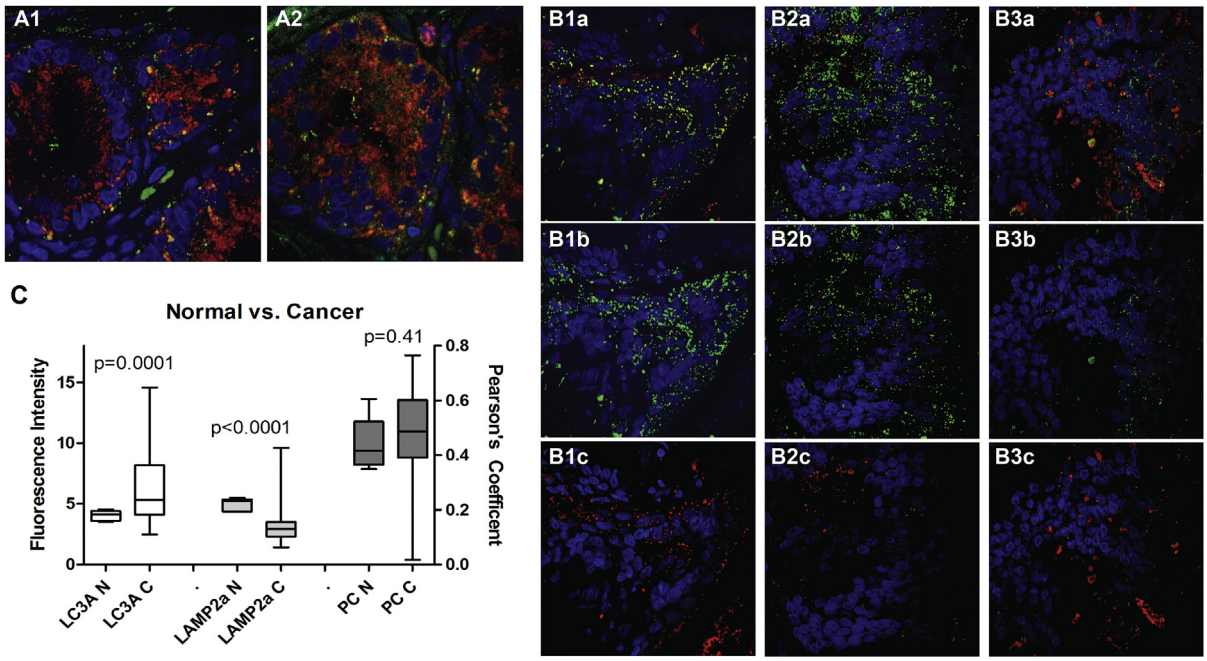

Fig. 1. A. Double immunofluorescence of normal prostate glands (A1, A2): intense expression of LAMP2a (red) and low expression of LC3A (green) in the epithelial cells. B. Double immunofluorescence of prostate cancer: (a), LC3A fluorescence (b; green) and LAMP2a fluorescence (c, red). Set of figures B1 show a typical case with intense LC3A and LAMP2a expression, as well as intense colocalization of the proteins. Set of figures B2 show a typical case with intense LC3A expression but low LAMP2a expression. Set of figures B3 show a case with normal-like expression patterns, with low LC3A and intense LAMP2a expression. C. Box and whiskers plot of the range and median value of the LC3A, LAMP2a fluorescence intensity, as well as of the Pearson's colocalization coefficient, in normal prostate glands vs. prostate carcinomas. (For interpretation of the references to color in this figure legend, the reader is referred to the web version of this article.)

of the pellet fraction of PC3 cell line showed intense presence of the membrane bound LC3A-II protein, in the context of low LAMP2a and p62/Sequestrosome protein levels, confirming intensified autophagic flux (Fig. 3B). In the DU145 cell line, the levels of LC3A remained low after irradiation, in the context of accumulation of the p62 and LAMP2a proteins, confirming a blockage of the autophagic flux. The western blot findings on the divergent between the two cell lines p62 expression response following irradiation was also confirmed in confocal microscopy (Fig. 3B). Western blot analysis of positive control cells treated with Bafilomycin showed intense accumulation of LC3A-II, LAMP2a and p62 proteins in both cell lines (Fig. 3A and B).

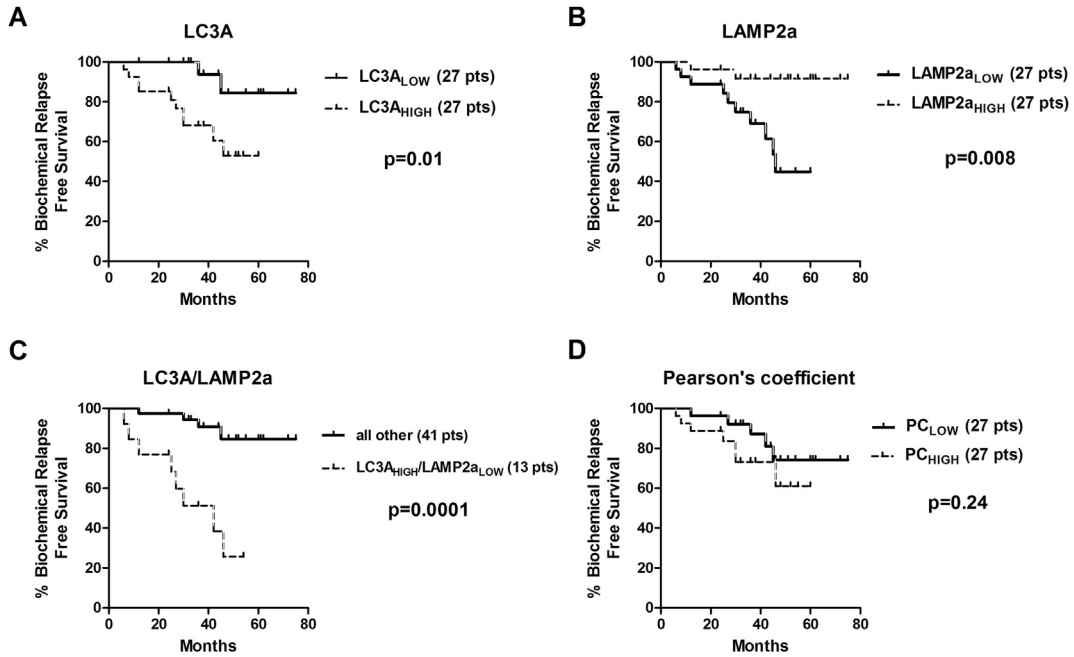

Fig. 2. Kaplan–Meier survival curves of the biochemical relapse free survival of prostate cancer patients treated with radical radiotherapy, stratified for LC3A, LAMP2a, double LC3A/LAMP2A expression and the Pearson's colocalization coefficient.

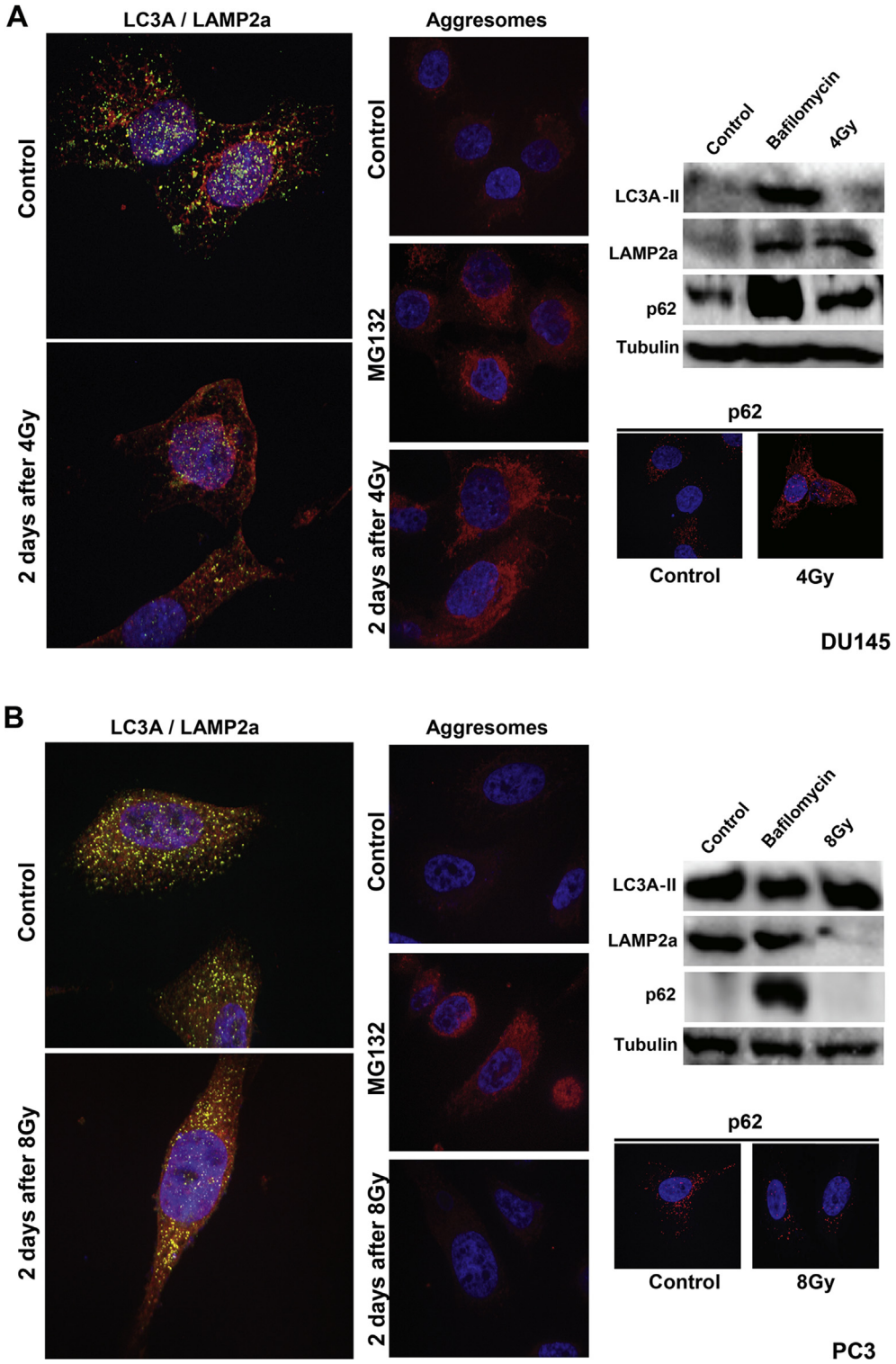

Fig. 3. Autophagy response of DU145 (A) and of PC3 (B) cell lines after exposure of cells to 4 Gy and 8 Gy of radiation, respectively. Colocalization of LC3A (green)/LAMP2a (red) is reduced in the DU145, while aggresomes and p62 are accumulated (confocal microscopy; A). In the PC3 cell line, the LC3A/LAMP2a robust colocalization persists, while no accumulation of aggresomes or p62 is evident (confocal microscopy; B). In western blots, LAMP2a and p62 levels are increased in the DU145 cell line, whilst reduced in the PC3 one, suggestive of reduced and increased lysosomal consumption, respectively. (For interpretation of the references to color in this figure legend, the reader is referred to the web version of this article.)

3.5. Autophagy blocking and radiosensitivity

DU145 cell line is far more radiosensitive than PC3. The dose demanded to obtain 50% survival as measured 8 days after irradiation is 4.80 and 10.3 Gy, respectively (Fig. 4A and C). Following silencing of the LC3A or the LAMP2a protein expression with specific siRNAs (Fig. 4B and D), an important radiosensitizing effect was evident for both cell lines (Fig. 4A and C).

4. Discussion

Autophagy is an important biological pathway that allows the clearance of damaged proteins and organelles at the same time providing the cell with fuel molecules to be used for its metabolical demands. Cancer cells have an intensified autophagic activity compared to normal cells, as shown in previous studies from our group in various human malignancies [10–12]. Regarding prostate cancer, overexpression of autophagy markers, like LC3A and Beclin 1, is common and characterizes a subgroup of patients with intensified anaerobic metabolism, high Gleason score and tumors with extraprostatic invasion [13].

The basal levels of autophagy flux may be an important feature that defines resistance of cancer cells to chemotherapy or targeted therapy, but published translational studies are scarce in the literature. Lymphomas with increased basal autophagy levels have been proved resistant to sorafenib therapy [14], a finding also confirmed in melanoma patients treated with sorafenib and temozolomide [15]. Colorectal cancer patients with high LC3 and Beclin 1 expression were resistant to cetuximab [16]. High basal levels of autophagy markers also defined poor response of breast cancer to trastuzumab based chemotherapy [17].

The role of base line autophagy activity in the outcome of cancer patients treated with radiotherapy, remains poorly investigated. Chen et al. found that LC3 and Beclin 1 overexpression defined poor survival of patients with esophageal cancer treated with chemo-radiotherapy [18]. Patients with Beclin 1 overexpressing nasopharyngeal cancer had also a poor post-radiotherapy outcome [19]. Prostate cancer is one of the most common human malignancies, treated worldwide with radiotherapy, but the role of autophagy in prostate cancer radioresistance has never been studied in the past.

In the current study, using double confocal immunofluorescense to detect the expression of LC3A (autophagosomal membranes) and of LAMP2a (lyosomal membranes) proteins, we showed that normal prostate glands had low levels of LC3A and high levels of LAMP2a expression. This is suggestive of low levels of autophagic flux (poor lysosomal consumption and low presence of LC3A autophagosomes). On the contrary, a large percentage of the prostate carcinomas examined showed a reverse expression pattern, with LC3A over- and LAMP2a under-expression, suggestive of intensified lysosomal consumption in the context of autophagosomal abundance, thus an intensified autophagy flux. Low Gleason score tumors exhibited most often autophagy expression patterns similar to the normal prostate gland epithelium. Tumors with high LC3A and low LAMP2a levels were resistant to radiotherapy, as shown by the poor biochemical relapse free survival of these patients.

In vitro studies were, thereafter, scheduled to further investigate these clinicopathological findings. We used two prostate cancer cell lines, the DU145 and the PC3, the later showing an impressive

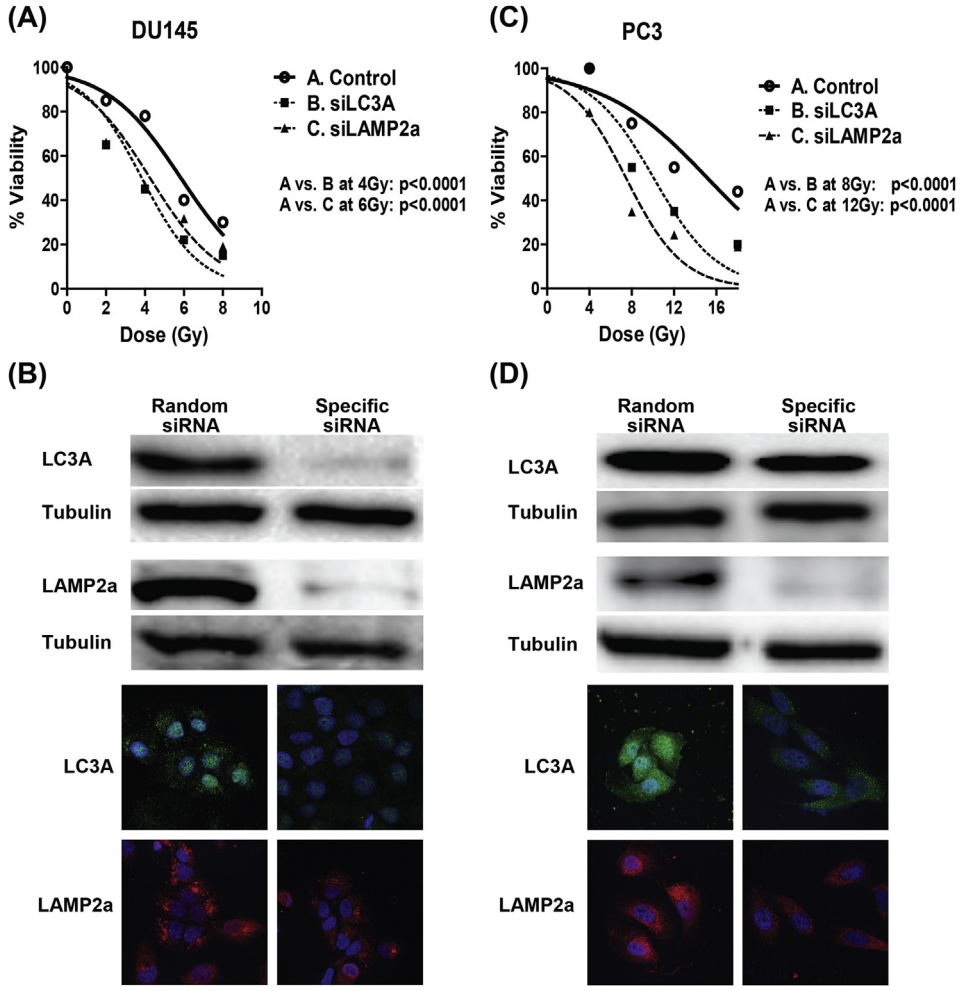

Fig. 4. Post-irradiation viability of DU145 and PC3 prostate cancer cell lines (A,C). Effective suppression of the LC3A or the LAMP2a gene expression (western blots and confocal images; B,D), resulted in important reduction of the cell viability in both cell lines (dose response curves; A,C).

resistance to radiotherapy. Irradiation of the DU145 cell line with 4 Gy resulted in a sharp blockage of the autophagic flux as shown by the accumulation of aggresomes and lysosomes in the cell cytoplasm. The p62 protein showed increased levels, thus low rates of its degradation due to poor auto-lysosomal fusion. On the contrary, the autophagy flux remained unaltered, if not intensified, after exposure of the radioresistant PC3 cells even to 8 Gy of radiation. This suggests that a functional autophagic machinery after irradiation reduces post-irradiation cell death, which is in accordance with a previous study on endothelial cell autophagic response to radiation [20]. By blocking LC3A or LAMP2a expression, both cell lines were sensitized. The suppression of LAMP2a reduces the production and concentration of LAMP2a+ lysosomes, resulting in decreased autophagosome consumption, reduction of the auto-lysosomal flux and increased sensitivity to radiation. The forced reduction of LAMP2a lysosomes in these experiments should not be confused with the poor LAMP2a expression found in the histopathological study, where this event is presumably a result of increased auto-lysosomal consumption leading to resistance to radiotherapy. The results from the histopathological and the experimental studies are in full accordance suggesting that increased LAMP2a/LC3A mediated autophagic flux goes along with radioresistance. Chang et al., also noted that reduction of autophagy by PI3K inhibitors contributed to the radiosensitizing effect of such compounds on prostate cancer cells [21]. Moreover, by impairing the autophagic flux through restoration of miR-205 expression, the sensitivity of hormone-resistant prostate cancer cells to cisplatin was enhanced [22].

We conclude that high base line autophagy activity and cell ability to sustain functional autophagic flux define resistance of prostate cancer cells to radiotherapy, which can be reversed by blocking LC3A or LAMP2a expression or eventually of any critical element in the chain of the autophagic machinery. The current data support the concept that the development of potent and selective autophagy inhibitors, targeting up-regulated components of the autophagy pathway in cancer cells, may prove of importance in the field of clinical radiotherapy.

Conflict of interest

None.

Acknowledgments

The study has been funded by the «Training and Lifelong Learning – Aristeia» project, code no 520, ESPA 2007–2013, GGET decision number 12605/26.09.2012.

Transparency document

Transparency document related to this article can be found online at http://dx.doi.org/10.1016/j.bbrc.2015.04.014.

References

[1] P.A. Kupelian, M. Elshaikh, V.A. Reddy, et al., Comparison of the efficacy of local therapies for localized prostate cancer in the prostate-specific antigen era: a large single-institution experience with radical prostatectomy and external-beam radiotherapy, J. Clin. Oncol. 20 (2002) 3376–3385.
[2] A. Baccala Jr., A.M. Reuther, F.J. Bianco Jr., et al., Complete resection of seminal vesicles at radical prostatectomy results in substantial long-term disease-free survival: multi-institutional study of 6740 patients, Urology 69 (2007) 536–540.
[3] R.M. Galalae, G. Kovács, J. Schultze, et al., Long-term outcome after elective irradiation of the pelvic lymphatics and local dose escalation using high-dose-rate brachytherapy for locally advanced prostate cancer, Int. J. Radiat. Oncol. Biol. Phys. 52 (2002) 81–90.
[4] S.E. Berry, T.J. Kinsella, Targeting DNA mismatch repair for radiosensitization, Semin. Radiat. Oncol. 11 (2001) 300–315.
[5] D.J. Klionsky, F.C. Abdalla, H. Abeliovich, et al., Guidelines for the use and interpretation of assays for monitoring autophagy, Autophagy 8 (2012) 445–544.
[6] C.E. Zois, M.I. Koukourakis, Radiation-induced autophagy in normal and cancer cells: towards novel cytoprotection and radio-sensitization policies? Autophagy 5 (2009) 442–450.
[7] A.M. Cuervo, J.F. Dice, Regulation of lamp2a levels in the lysosomal membrane, Traffic 1 (2000) 570–583.
[8] M.I. Koukourakis, A. Papadopoulou, I. Abatzoglou, et al., Postoperative pelvic hypofractionated accelerated radiotherapy with cytoprotection (HypoARC) for high-risk or recurrent prostate cancer, Anticancer Res. 32 (2012) 4561–4568.
[9] M.A. Zachari, P.S. Chondrou, S.E. Pouliliou, et al., Evaluation of the alamarblue assay for adherent cell irradiation experiments, Dose Response 12 (2013) 246–258.
[10] A. Giatromanolaki, E. Sivridis, A. Mitrakas, et al., Autophagy and lysosomal related protein expression patterns in human glioblastoma, Cancer Biol. Ther. 15 (2014) 1468–1478.
[11] E. Sivridis, A. Giatromanolaki, V. Liberis, et al., Autophagy in endometrial carcinomas and prognostic relevance of 'stone-like' structures (SLS): what is destined for the atypical endometrial hyperplasia? Autophagy 7 (2011) 74–82.
[12] E. Sivridis, M.I. Koukourakis, C.E. Zois, et al., LC3A-positive light microscopy detected patterns of autophagy and prognosis in operable breast carcinomas, Am. J. Pathol. 176 (2010) 2477–2489.
[13] A. Giatromanolaki, E. Sivridis, S. Mendrinos, et al., Autophagy proteins in prostate cancer: relation with anaerobic metabolism and Gleason score, Urol. Oncol. 32 (2014), 39.e11-8.
[14] A. Guidetti, C. Carlo-Stella, S.L. Locatelli, et al., Phase II study of sorafenib in patients with relapsed or refractory lymphoma, Br. J. Haematol. 158 (2012) 108–119.
[15] X.H. Ma, S. Piao, D. Wang, et al., Measurements of tumor cell autophagy predict invasiveness, resistance to chemotherapy, and survival in melanoma, Clin. Cancer. Res. 17 (2011) 3478–3489.
[16] G.F. Guo, W.Q. Jiang, B. Zhang, et al., Autophagy-related proteins Beclin-1 and LC3 predict cetuximab efficacy in advanced colorectal cancer, World J. Gastroenterol. 17 (2011) 4779–4786.
[17] M.I. Koukourakis, A. Giatromanolaki, A. Bottini, et al., Prospective neoadjuvant analysis of PET imaging and mechanisms of resistance to Trastuzumab shows role of HIF1 and autophagy, Br. J. Cancer 110 (2014) 2209–2216.
[18] Y. Chen, X. Li, X. Wu, et al., Autophagy-related proteins LC3 and Beclin-1 impact the efficacy of chemoradiation on esophageal squamous cell carcinoma, Pathol. Res. Pract. 209 (2013) 562–567.
[19] X.B. Wan, X.J. Fan, M.Y. Chen, et al., Elevated Beclin 1 expression is correlated with HIF-1alpha in predicting poor prognosis of nasopharyngeal carcinoma, Autophagy 6 (2010) 395–404.
[20] D. Kalamida, I.V. Karagounis, A. Giatromanolaki, et al., Important role of autophagy in endothelial cell response to ionizing radiation, PLoS One 9 (2014) e102408.
[21] L. Chang, P.H. Graham, J. Hao, et al., PI3K/Akt/mTOR pathway inhibitors enhance radiosensitivity in radioresistant prostate cancer cells through inducing apoptosis, reducing autophagy, suppressing NHEJ and HR repair pathways, Cell Death Dis. 5 (2014) e1437.
[22] M. Pennati, A. Lopergolo, V. Profumo, et al., miR-205 impairs the autophagic flux and enhances cisplatin cytotoxicity in castration-resistant prostate cancer cells, Biochem. Pharmacol. 87 (2014) 579–597.